Circular RNAs accumulate in ageing human placental tissue and in stillbirth, leading to DNA damage and cellular senescence

Anya L. ARTHURS[a,b,k*], Matilda R. JACKSON[c,d,e], Dylan McCULLOUGH[a,b], Hamish S. SCOTT[c,d,f,g,h], Christopher P. BARNETT[f,i], Stuart T. WEBB[a,b,c], Melanie D. SMITH[a,b], Tanja JANKOVIC-KARASOULOS[a,b], Gustaaf A. DEKKER[j], Claire T. ROBERTS[a,b].

[a] Flinders Health and Medical Research Institute, Flinders University, Adelaide, South Australia, Australia 5042

[b] College of Medicine and Public Health, Flinders University, Adelaide, South Australia, Australia 5042

[c] Department of Genetics and Molecular Pathology, SA Pathology, Adelaide, South Australia, Australia 5000

[d] Centre for Cancer Biology, an alliance between SA Pathology and University of South Australia, Adelaide, South Australia, Australia 5000

[e] Australian Genomics, Parkville, Victoria, Australia

[f] Adelaide Medical School, The University of Adelaide, Adelaide, South Australia, Australia 5000

[g] ACRF Genomics Facility, Centre for Cancer Biology, an alliance between SA Pathology and University of South Australia, Adelaide, South Australia, Australia 5000

[h] UniSA Clinical and Health Sciences, University of South Australia, Adelaide, South Australia, Australia 5000

[i] Paediatric and Reproductive Genetics Unit, South Australian Clinical Genetics Service, Women's and Children's Hospital, North Adelaide, South Australia, Australia 5000

[j] Department Obstetrics and Gynecology, Lyell McEwin Hospital, The University of Adelaide, Adelaide, South Australia 5112

[k] School of Biomedicine and Robinson Research Institute, The University of Adelaide, Adelaide, South Australia, Australia 5000

* Corresponding author: anya.arthurs@flinders.edu.au

Disclosure Statement

Provisional patent (A.L.A, C.T.R) # 2024902762, filed 2nd September 2024. The remaining authors report no conflict of interest.

Condensation page

Tweetable Statement: Stillbirth is associated with premature placental ageing; this may be due to accumulation of circular RNA molecules which cause DNA breaks and induce cellular senescence.

Short title: Circular RNAs, Placental Ageing and Stillbirth

AJOG at a Glance:

A. This study was conducted to confirm premature placental ageing in cases of unexplained stillbirth, and to investigate the role of circular RNAs in the process of placental ageing.
B. Circular RNAs accumulate in ageing healthy placenta and accumulate prematurely in stillbirth placentae. Circular RNAs bind directly to placental DNA, inducing DNA breaks and cellular senescence, thereby contributing to overall functional decline of the placenta, reducing its ability to support the fetus. Circular RNAs in maternal blood represents a novel screening tool for detection of stillbirth risk.
C. Premature placental ageing has previously been associated with stillbirth, however circular RNAs have never before been implicated in this process. Circular RNA accumulation in ageing tissues has been shown in model species (i.e. *C. elegans, Drosophila Melanogaster*, mice) but this is the first evidence in human tissues and in the placenta.

Word count: 5091

Graphical Abstract

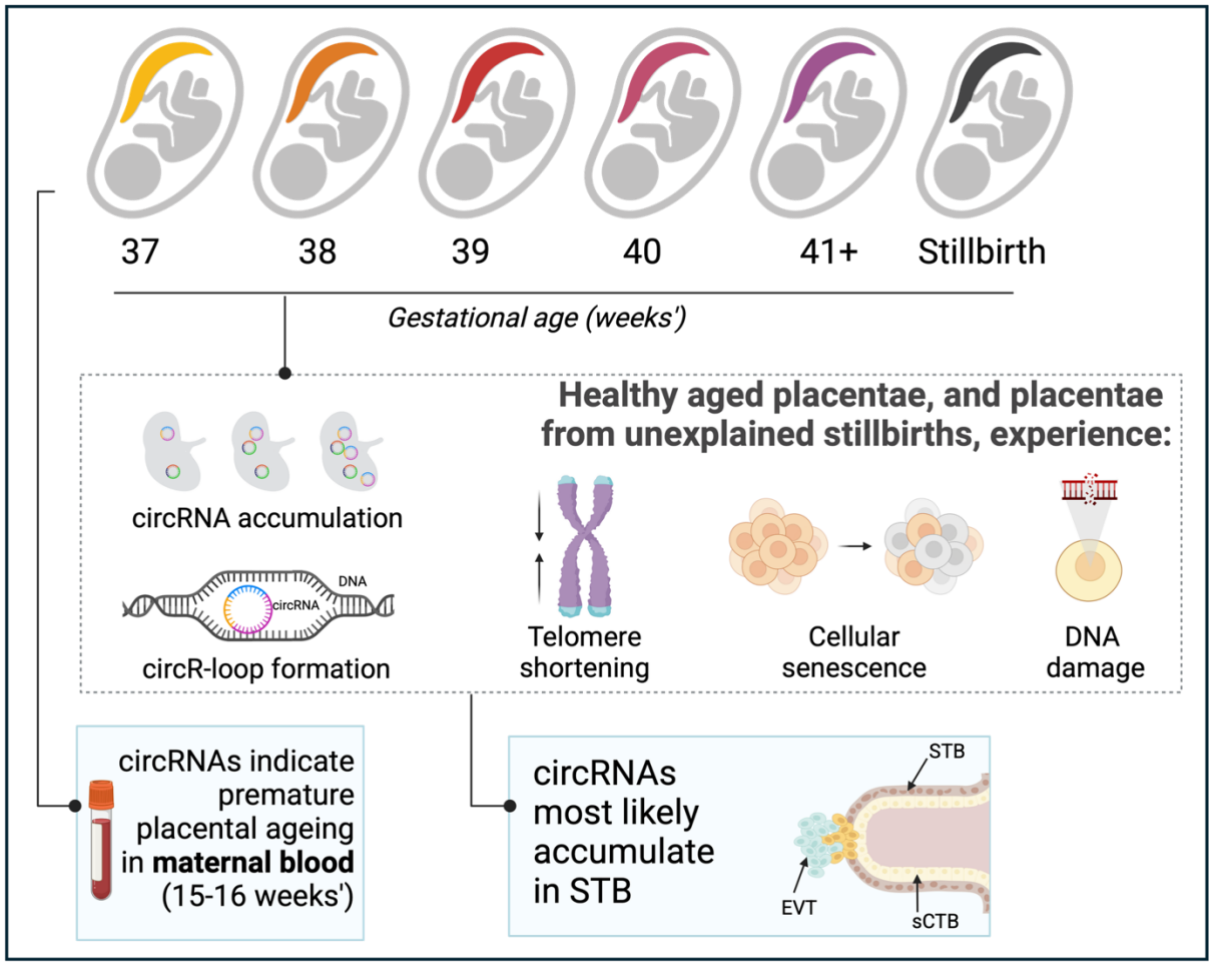

* STB = syncytiotrophoblast; EVT = extravillous trophoblast; sCTB = subsyncytial cytotrophoblast.

Keywords: stillbirth, placenta, pregnancy, ageing, DNA, circular RNA, double stranded breaks, senescence, telomere

Structured Abstract

Background: Unexplained stillbirth may occur due to premature placental ageing, with unexpected deterioration of placental function for gestational age. Circular RNAs (circRNAs) are enzyme-resistant RNA molecules that accumulate in ageing tissues. Furthermore, circRNAs bind gDNA directly, forming circRNA:DNA complexes which can induce DNA breaks and genomic instability.

Objectives: This study investigated tissue ageing and circRNA accumulation with gestational age in healthy and stillbirth placentae, and determined whether circRNAs directly interact with placental DNA causing DNA damage and cellular senescence.

Study design: Placenta samples (n=60 term uncomplicated; n=4 unexplained stillbirth, 23, 26, 31, 34 weeks' gestation) were assessed. Abundance of 7 candidate circRNAs (circ_0009000, circ_0024157, circ_0061017, circ_0036877, circ_0054624, circ_0111277 and circ_0000284), and their linear transcripts, was quantified using qPCR. Total RNA, in the presence and absence of RNase R and RNase H1, was determined using the Qubit fluorimeter. Physical interaction of candidate circRNAs with DNA was confirmed by DNA:RNA ImmunoPrecipitation (DRIP)-qPCR. Telomere length was assessed using real-time PCR. Relative abundance of senescence-associated genes was quantified using qPCR. DNA damage was assessed using an alkaline Comet Assay. Patient-derived trophoblast stem cells (TSCs) differentiation into syncytiotrophoblasts or extravillous trophoblasts was confirmed using immunofluorescence microscopy. The effect of circ_0000284 knockdown was assessed following transfection with either a siRNA (designed to knockdown circ_0000284) or a scrambled siRNA control, at 5, 10 and 20 nM final concentrations using Lipofectamine RNAiMax. Abundance of circRNAs in maternal blood sampled between 15-16 weeks' gestation (n=12 control, n=6 women who went

on to have a stillbirth) was determined using qPCR. Appropriate statistical analyses were undertaken (SPSS).

Results: Placental DNA damage, senescence and expression of 7 candidate circRNAs, but not their linear transcripts, were increased in 40 and 41+ weeks' gestation samples, and in stillbirth, compared with earlier gestations (37-39 weeks'). DRIP-qPCR signal size was significantly larger in term placentae than in enzyme-treated controls, confirming that all candidate circRNA loci bind to placental DNA. Abundance of circRNA was significantly decreased with the addition of RNase H1, compared with all healthy gestation samples, indicating that stillbirth placentae may lack RNase H1. Telomere length is shorter in placentae from stillbirths compared with healthy 37 weeks' placentae. Depletion of circ_0000284 by specific siRNA in primary cells significantly reduced DNA damage and increased expression of senescence-associated genes compared to control. Abundance of candidate circRNAs are increased in maternal blood at 16 weeks' gestation for women who went on to have a stillbirth compared with women who had live births.

Conclusions: Stillbirth placentae show accelerated ageing with shortened telomeres, premature DNA breaks, increased cellular senescence and accumulation of candidate circRNAs, at levels consistent with older gestation tissue. These circRNAs bind to DNA in the placenta, and circ_0000284 knockdown reduces DNA breaks and senescence in primary placental cells. Therefore, circRNAs play a role in placental ageing and associate with stillbirth, likely via decreased RNase H1 abundance, preventing circRNA degradation and facilitating circRNA accumulation, and subsequent circR-loop formation. circRNAs present a viable method of stillbirth risk screening.

110 # 1. Introduction

111 Stillbirth is defined as a fetal death prior to birth of a baby of either (i) ≥20 completed weeks'
112 of gestation or, (ii) ≥400g birthweight[1]. Annually there are 2 million stillbirths worldwide[2],
113 with ~2300 occurring every year in Australia, at a rate unchanged for decades[1]. Whilst some
114 cases of stillbirth can be attributed to fetal congenital abnormalities, many cases of stillbirth
115 are "unexplained", where autopsy that includes fetal genetics does not establish cause.
116 Although some risk factors have been identified[1,3], the aetiology of unexplained stillbirth is
117 unknown, and is thus impossible to prevent. One theory for the mechanism underpinning
118 unexplained stillbirth is premature placental ageing.
119

120 The placenta is a transient organ with a finite life in gestation. Placental ageing is a normal
121 phenomenon resulting in physical changes in late gestation without fetal compromise.
122 Accelerated placental ageing can occur in stillbirth, leading to reduced placental functional
123 capacity for fetal support. Whilst markers of tissue ageing, including measures of telomere
124 length[4] and DNA damage[3-5], are reportedly irregularly high in stillbirth placentae, a direct
125 measure of DNA breaks has not previously been reported.

126

127 Tissue ageing has been associated with circular RNAs (circRNAs). circRNAs can be generated
128 from most genes and encompass one or multiple exonic or intronic regions of RNA.
129 Importantly, they display tissue-specific patterns of expression, making them unique to their
130 tissue of origin as well as the genome of the individual. circRNAs are inherently stable, hence
131 they can accumulate in tissues with age (previously shown in *Drosophila melanogaster,*
132 *Caenorhabditis elegans* and murine models[6-8]).

133

134 Whilst circRNAs have many functions[9], of importance is their ability to directly bind to
135 genomic DNA, forming a circRNA:DNA complex (termed a 'circR-loop')[10]. Due to the steric
136 hinderance, the presence of a circR-loop can cause RNA polymerase II to stall during
137 transcription, subsequently leading to a double-stranded DNA break. This often results in
138 genomic instability[11], cellular senescence[12] and cell death[13]. Whilst their circular form makes
139 them difficult to degrade, RNase H1 can potentially degrade specific circRNAs which form
140 circR-loops, as these maintain a locally open secondary structure[14] (e.g. ci-ankrd52[15]).
141

142 Given that unexplained stillbirth may be due to premature placental ageing, and that circRNAs
143 accumulate in ageing animal tissues, we sought to determine whether circRNAs accumulated
144 with gestational age in healthy and stillbirth placentae. We further investigated whether select
145 circRNAs bind to DNA to form circR-loops and induce DNA breaks. We performed *in vitro*
146 experiments to determine the role of circ_0000284 in contributing to placental cell senescence
147 and DNA damage. Finally, we investigated the potential use of circRNAs as a screening tool
148 for placental ageing culminating in unexplained stillbirth. This study provides novel evidence
149 of circRNA accumulation in ageing human tissue and proposes a potential mechanism for
150 stillbirth pathogenesis.

151 # 2. Methods

152 ## 2.01 Tissue Samples

153 *First trimester (6–8 weeks' gestation) human placentae:* were obtained with informed consent
154 from women undergoing elective termination of pregnancy at the Pregnancy Advisory Centre
155 in the Queen Elizabeth Hospital, in Woodville, South Australia. Ethics approval was obtained
156 from the Central Adelaide Local Health Network Human Research Ethics Committee,
157 HREC/16/TQEH/33, Q20160305. Placentae were collected within minutes of termination
158 upon which villus tissue was washed with Hanks' Balanced Salt Solution (HBSS; Gibco,
159 Sigma-Aldrich) and transported to the laboratory on ice.

160 *Healthy placentae from 37-41+ weeks' gestation:* Term placentae were obtained at the Lyell
161 McEwin Hospital in Elizabeth, South Australia, from women recruited as part of the Screening
162 Tests to predict poor Outcomes of Pregnancy (STOP) (2015–2018) cohort study[16]. The study
163 was registered with the Australian and New Zealand Clinical Trials Registry (ACTRN
164 12614000985684). All placentae were associated with uncomplicated pregnancies and were
165 collected from white women. Tissue biopsies from placentae were washed in phosphate-
166 buffered saline (PBS) before being snap frozen and held in liquid nitrogen for 15 min, then
167 stored at -80°C. Ethics approval was obtained from the Women's and Children's Health
168 Network Human Research Ethics Committee (HREC/14/WCHN/90; STOP). All women
169 provided written informed consent.

170 *Placentae collected from unexplained stillbirths:* Small placental biopsies from unexplained
171 stillbirth cases were obtained from women who had been recruited in to the NHMRC- and
172 GHFM-MRFF-funded Genomic Autopsy Study[17]. Placental biopsies were obtained as part of

173 the standard autopsy procedure and were stored at -80°C as approved by the Human Ethics
174 Committee of the Women's and Children's Health Network, South Australia, Australia
175 (HREC/15/WCHN/35) and Melbourne Health as part of the Australian Genomics Health
176 Alliance protocol (HREC/16/MH/251). Informed consent was obtained to allow access to
177 relevant medical information and subsequent storage of anonymized samples, genomic data
178 and/or medical information in relevant databases and publications.

179 *Maternal blood samples collected at 15-16 weeks' gestation:* peripheral non-fasting blood
180 samples were collected as part of the STOP cohort study (see above) and placed on ice prior to
181 processing to isolate plasma. Samples were then stored at -80°C prior to subsequent analyses.

182

183 **2.02 Isolation and cultivation of trophoblast stem cells (TSCs)**

184 TSCs were isolated from n=5 first-trimester placentae as previously described[18,19]. Briefly,
185 first-trimester villus tissue was washed in HBSS (4 °C) prior to manually isolating villus
186 structures for further processing. Villi in HBSS were centrifuged (1000 rpm, 1 min) prior to
187 three consecutive enzymatic digest steps and density gradient centrifugation as per Haider *et*
188 *al.*[20]. After careful collection of cells between the 35% and 50% Percoll layers, cells were
189 thoroughly washed with HBSS before seeding in fibronectin-coated (20 µg/mL; Millipore)
190 culture plates using a culture medium to promote stemness (media details in **Table 1**). Cells
191 were cultured for 14 days in humidified incubators at 37°C, 1% O_2 in 5% CO_2 (to mimic the *in*
192 *utero* first-trimester placental oxygen tension) prior to differentiation to syncytiotrophoblast or
193 extravillous trophoblast lineages.

194

195 **2.03 Differentiation of TSCs into syncytiotrophoblast and extravillous**
196 **trophoblast lineages**

197 Patient-derived TSCs were reprogrammed to syncytiotrophoblast or extravillous trophoblast
198 lineages using specific culture media as described in Tan *et al.*[21] (listed in **Table 1**). TSCs were
199 plated in 6-well plates and cultured in syncytiotrophoblast reprogramming media or
200 extravillous trophoblast reprogramming media for a total of four passages. Passaging was
201 completed using TrypLE Express (Gibco) according to manufacturer's instructions and cells
202 were replated at a density of ~20% (1:5 dilution) per well. At the time of each passage, a portion
203 of cells were harvested in liquid nitrogen for downstream qPCR analyses. At the end of passage
204 4 culture, cells were fixed for visualisation or harvested in liquid nitrogen for further
205 experiments.

206

207 **2.04 siRNA transfection of TSCs**

208 TSCs were reprogrammed to syncytiotrophoblasts as above (see **2.03**). siRNA sequence was
209 designed to be complementary to the backsplice junction of circ_0000284 (sequence:
210 ctttattcgagtgattatgattgccatt; scrambled siRNA sequence: tctatcattcatggtatctgtgtatgat). siRNA
211 was produced by Thermo Fisher Scientific (Silencer Select siRNA). Cells were transfected (24-
212 well plates) with the siRNA and scrambled siRNA at 5, 10 and 20 nM final concentrations
213 using Lipofectamine RNAiMAX (Life Technologies) following the manufacturer's
214 instructions. After optimisation, experiments proceeded with 10 nM final concentration (as the
215 lowest siRNA concentration producing the desired level of knockdown). At 96 hours post-
216 siRNA transfection cells were collected and either (i) immediately used for Comet assay or (ii)
217 snap frozen in liquid nitrogen prior to storage at −80°C for subsequent RNA analyses.

218

219 **2.05 RNA Extraction**

220 *Placenta tissue:* Healthy term and stillbirth placental tissues (25mg) were weighed and washed
221 with phosphate-buffered saline (PBS). Tissue was disrupted by homogenizing for 3.5 min at
222 30 Hz (TissueLyser, QIAGEN) in 1mL *TRIzol Reagent* (Sigma-Aldrich). Cultured patient-
223 derived cells were suspended in 1mL *TRIzol Reagent*. The manufacturer's protocol was then
224 followed to isolate total RNA. The purity and integrity of extracted RNA samples were
225 determined using the Qubit 2.0 fluorometer (Thermo Fisher Scientific). Samples from term and
226 stillbirth placenta tissues were then split into two aliquots, with one aliquot to be assessed for
227 circRNA expression levels and the other to be assessed for linear transcript expression levels.
228 Samples to be assessed for circRNA expression levels were heated to 70°C for 5 mins, then

229 immediately cooled below 40°C before incubation with RNase R (10U / reaction; Astral
230 Scientific) for 1 h at 40°C. This step was essential to digest all linear RNAs, leaving only lariat
231 or circular RNA structures.

232 *Maternal blood:* Total RNA was isolated from 200 µL thawed frozen plasma using the
233 miRNeasy Serum/Plasma kit (Qiagen), according to manufacturer's instructions and as per
234 Vilades, *et al.*[22]).

235

236 **2.06 RNA Quantification**

237 Total RNA for each sample from term and stillbirth placenta tissues, after incubation of 1 µg
238 of RNA either with RNase R or untreated, was quantified using the Qubit 2.0 fluorimeter
239 (Thermo Fisher Scientific). Total RNA from maternal blood samples was quantified using the
240 Qubit 2.0 fluorimeter as is. As per Drula, *et al.*[23], Qubit measurement was accomplished with
241 the Qubit™ RNA High Sensitivity (HS) assay kit using 1 µL of the RNA sample, 198 µL of
242 the kit Qubit working solution and 1 µL of the provided fluorophore, as per manufacturer's
243 instructions. RNA amount was normalised based on the standard curve and input and compared
244 between RNase R treated and untreated groups, in the presence and absence of RNase H1-
245 specific siRNA (as per Wu, *et al.*[24]) per sample to quantify bulk circRNA abundance.

246

247 **2.07 cDNA Synthesis and Quantitative Polymerase Chain Reaction (qPCR)**

248 Synthesis of complementary DNA (cDNA) was conducted beginning with 1µg of total RNA
249 using the QuantiNova Reverse Transcription Kit (QIAGEN) according to the manufacturer's

250 protocol. qPCR was performed in triplicate and conducted with SYBR Green (QIAGEN)
251 according to manufacturer's instructions, with *YWHAZ, GAPDH* and *ACTB* as housekeeping
252 genes (all primer sequences in **Table 2**). Custom divergent primers were designed for each
253 circRNA, flanking the backsplice junction, with an amplicon size <300 base pairs. As an
254 additional confirmation of amplification specificity, all primers were assessed using the Primer
255 design BLAST tool[23]. Furthermore, primer specificity was confirmed via melt curve analysis
256 from qRT-PCR. The qPCR conditions were PCR initial activation at 95°C for 5 min followed
257 by 50 cycles of 95°C for 15s, T_m (detailed in **Table 2**) for 40s and 72°C for 20s. qPCR results
258 were analysed using the 2-ΔΔCT method[25]. Samples were sorted into groups depending on
259 gestational age of tissue (see **Table 3** for numbers and characteristics of women's samples
260 used).

261

262 **2.08 Telomere length analysis**

263 Genomic DNA was extracted from samples using the DNeasy Blood and Tissue Kit (Qiagen)
264 starting with 25 mg tissue. Telomere length was assessed according to the optimised protocol
265 outlined by Cawthon, 2009[26]. Standard curves were generated for telomere lengths from single
266 copy gene amplifications using a reference DNA. The telomere length for each sample was
267 derived based on the ratio of telomere length between the sample and single copy gene standard
268 (*T*/*S* ratio).

269

270 **2.09 Comet Assay**

271 The Abcam Comet Assay Kit (ab238544; Abcam) was used to assess DNA damage in isolated
272 trophoblasts, as per manufacturer's instructions. For each sample from term and stillbirth
273 placenta tissues, approximately 25 mg tissue (stored at -80°C) was used. For each sample from
274 cultured early gestation patient samples, $2.5x10^5$ cells were used. Alkaline electrophoresis was
275 performed. The DNA integrity of 100 cells per placenta was analysed using CometScore 2.0
276 software (RexHoover.com). The fluorescence intensity of the comet 'tail' was used as a
277 measure of DNA damage (indicated as tail DNA%). Tail DNA was shown as a percentage
278 increase in damage relative to averaged control samples.

279

280 **2.10 DNA:RNA ImmunoPrecipitation (DRIP)**

281 DRIP was performed according to steps 3-25 in the protocol published by Sanz, *et al.* 2019[27],
282 with some notable exceptions for where tissue was used as a starting material instead of
283 cultured cells. Tissue was first prepared as follows before progressing to step 3 of the protocol.

284

285 Approximately 50mg frozen placental villous tissue was submerged in 1mL RLT+ buffer
286 (QIAGEN) with added 0.01% (v/v) β-mercaptoethanol and 0.5% (v/v) Reagent DX (QIAGEN)
287 with 1g beads. Tissue was disrupted by homogenizing for 3.5 min at 30 Hz (TissueLyser,
288 QIAGEN). Cell suspensions were centrifuged (3 min, max speed, 4°C) prior to removal of the
289 supernatant. The cell pellet was washed (sterile DPBS, 5mL) before centrifugation (3 min,
290 1000 RPM, 4°C) and removal of the supernatant. Steps 3-25 of the protocol[27] were then
291 followed.

292

293 **2.11 Immunocytochemistry of cultured TSCs**

294 Immunocytochemistry was performed as described by Morosin *et al.*, 2020[28]. Briefly, fixed
295 cells were permeabilised in 0.1% Triton X-100 in PBS (Bio-Rad) before blocking in 1% BSA.
296 Cells were either incubated with E-cadherin primary antibody (Abcam ab1416;
297 syncytiotrophoblast lineage only) or a HLA-G primary antibody (Invitrogen MA1-10359;
298 extravillous trophoblast lineage only) before being washed with PBS and incubated with Alexa
299 Fluor 488 goat anti-mouse IgG (H+L) secondary antibody (Thermofisher, A-11001). Negative
300 controls were included where cells were incubated in the absence of either the primary antibody
301 or both the primary and secondary antibodies. Cells were mounted onto microscope slides
302 using a DAPI mounting medium (ProLong™ Diamond Antifade Mountant with DAPI;
303 Invitrogen). Slides were stored at 4°C and three images were taken per slide (imaged areas
304 were selected at random) using confocal microscopy at 40× magnification.

305 Syncytialisation was observed where multiple nuclei (blue) existed within one E-cadherin
306 boundary (green). Cells were classed as extravillous trophoblasts where HLA-G was expressed.

307

308 **2.12 Statistical Analysis**

309 Statistical analysis for differences between groups for qPCR and Comet Assay data was
310 undertaken using SPSS Statistics Software. Outliers were removed from the data using a
311 Grubbs' test. Data were assessed for normality distribution and either a Kruskal-Wallis test or
312 two-way ANOVA tests conducted. Adjustments were made for multiple comparisons
313 (Tukey's). Differences between groups were considered significant at $p<0.05$.

3. Results

3.01 Cohort Characteristics

Placenta samples were available from n=60 women who had healthy pregnancies (n=12 per gestational group) and n=4 women who experienced stillbirth. All stillbirths had been assessed by clinical pathologists as "unexplained fetal deaths", with no noted congenital anomalies.

Maternal and birth characteristics are presented in **Table 3**.

3.02 Abundance of candidate circRNAs in placenta across term and in stillbirth

Relative abundance of circ_0009000, expressed as fold change compared to abundance in placentae at 37 weeks' gestation, was significantly increased in placentae from 40 compared with 37 and 38 weeks' gestation (p_{37}=0.0005, p_{38}=0.0079; **Figure 1A**) and 41+ compared with 37 and 38 weeks' gestation (all p<0.0001), as well as in placentae from stillbirths compared with 37 and 38 weeks' gestation (p_{37}<0.0001, p_{38}=0.0006).

Relative abundance of circ_0024157 was significantly increased in placentae from 40 compared with 37 weeks' gestation (p=0.0003; **Figure 1B**) and 41+ compared with 37, 38 and 39 weeks' (p_{37}<0.0001, p_{38}=0.0002, p_{39}=0.0124), as well as in placentae from stillbirths compared with 37, 38 and 39 weeks' gestation (p_{37}<0.0001, p_{38}=0.0027, p_{39}=0.0336).

333 Relative abundance of circ_0061017 was significantly increased in placentae from 39
334 compared with 37 weeks' gestation (p=0.0260; **Figure 1C**), 40 compared with 37 and 38
335 weeks' gestation (p_{37}<0.0001, p_{38}=0.0053) and 41+ compared with 37 and 38 weeks' gestation
336 (p_{37}<0.0001, p_{38}=0.0003), as well as in placentae from stillbirths compared with 37 and 38
337 weeks' gestation (p_{37}<0.0001, p_{38}=0.0034).

338

339 Relative abundance of circ_0036877 was significantly increased in placentae from 39
340 compared with 37 weeks' gestation (p=0.0151; **Figure 1D**), 40 compared with 37 weeks'
341 gestation (p=0.0002) and 41+ compared with 37 and 38 weeks' gestation (all p<0.0001), as
342 well as in placentae from stillbirths compared with 37 and 38 weeks' gestation (p_{37}< 0.0001,
343 p_{38}=0.0038).

344

345 Relative abundance of circ_0054624 was significantly increased in placentae from 40
346 compared with 37 and 38 weeks' gestation (p_{37}<0.0001, p_{38}=0.0232; **Figure 1E**) and 41+
347 compared with 37, 38 and 39 weeks' gestation (p_{37}<0.0001, p_{38}<0.0001, p_{39}=0.0138), as well
348 as in placentae from stillbirths compared with 37 and 38 weeks' gestation (p_{37}<0.0001,
349 p_{38}=0.0012).

350

351 Relative abundance of circ_0111277 was significantly increased in placentae from 39
352 compared with 37 weeks' gestation (p=0.0443; **Figure 1F**), 40 compared with 37 weeks'
353 gestation (p=0.0002) and 41+ compared with 37, 38 and 39 weeks' gestation (p_{37}<0.0001,
354 p_{38}=0.0003, p_{39}=0.0050), as well as in placentae from stillbirths compared with 37 and 38
355 weeks' gestation (p_{37}<0.0001, p_{38}=0.0142).

356

357 Relative abundance of circ_0000284 was significantly increased in placentae from 40
358 compared with 37 weeks' gestation (p<0.0001; **Figure 1G**) and 41+ compared with 37, 38 and
359 39 weeks' gestation (p_{37}<0.0001, p_{38}<0.0001, p_{39}=0.0158), as well as in placentae from
360 stillbirths compared with 37 and 38 weeks' gestation (p_{37} < 0.0001, p_{38} = 0.0042).

361

362 **3.03 Candidate circRNAs bind to DNA to create circR-loops in term placentae**

363 DRIP-qPCR was used to detect circR-loops (DNA:RNA complexes; **Figure 1H**) in pooled
364 placenta samples from gestations 37-41+ weeks', to determine whether circRNAs which
365 accumulate in the ageing placenta interact directly with DNA.

366

367 After completing DRIP (see Methods), DRIP-qPCR analysis was undertaken using either
368 predesigned primers[27] for known R-loop-positive loci *TFPT* and *CALM3*, and known R-loop-
369 negative locus *EGFR1neg*, or using custom-designed primers (sequences listed in Methods) to
370 target the backsplice junctions of circ_0009000, circ_0024157, circ_0061017, circ_0036877,
371 circ_0054624, circ_0111277 and circ_0000284. All DRIP-qPCR analyses were completed
372 both in samples treated with and without RNase H treatment prior to DRIP. As RNase H
373 cleaves the RNA of RNA:DNA hybrids, it is expected that addition of RNase H to the sample
374 will result in a significantly suppressed R-loop signal and hence, a reduced DRIP-qPCR signal
375 (functioning as a negative control). This was confirmed in our results.

376

377 According to Sanz, *et al.*[27], R-loop positive loci are typically recovered with an efficiency
378 ranging from 1-15% of total input, whereas negative loci are typically recovered with values
379 of <0.1%. This was replicated in our results for placenta tissue **(Figure 1I)**, where *TFPT* (mean
380 11.499%, p=0.0008) and *CALM3* (mean 8.644%, p=0.0009) produced DRIP-qPCR signals,
381 shown as a % of total DRIP input, significantly larger than their RNase H-treated controls.
382 There was no significant difference between the DRIP-qPCR signals of *EGFR1neg* (mean
383 0.389%) with and without RNase H treatment.

384

385 DRIP-qPCR signal for circ_0009000 (mean 0.173%; **Figure 1J**), circ_0024157 (mean
386 0.166%), circ_0061017 (mean 0.172%), circ_0036877 (mean 0.169%), circ_0054624 (mean
387 0.173%), circ_0024157 (mean 0.177%) and circ_0000284 (mean 0.163%) was significantly
388 larger than their RNase H-treated controls (all p<0.0001).

389

390 3.04 circRNAs which accumulate in ageing placenta, and in stillbirth placenta, 391 are subject to RNase H1 degradation

392 One proposed method for endogenous circRNA degradation is via RNase H1[15], specifically for
393 circRNAs which can form circR-loops with template DNA due to their locally open secondary
394 structure. RNase H1 cleaves the circR-loop and, in some cases, further degrades the circRNA.

395

396 We assessed whether circRNAs in placenta samples from uncomplicated and stillbirth
397 placentae were subject to RNase H1 degradation. Quantity of total RNA for each sample was

398 unchanged with administration of an siRNA which specifically targets RNase H1 (**Figure 1K**).
399 For samples taken from uncomplicated pregnancies delivering at 37, 38, 39, 40 and 41+
400 weeks', and in stillbirth placentae, quantity of circRNA (after total RNA treatment with RNase
401 R) was significantly decreased with administration of the RNase H1-specific siRNA ($p<0.05$).
402 Furthermore, quantity of circRNAs was significantly lower after administration of RNase H1-
403 specific siRNA in placentae from stillbirths compared with all other gestations ($p_{37}=0.0094$;
404 $p_{38}=0.0087$; $p_{39}=0.0072$; $p_{40}=0.0090$; $p_{41+}=0.0099$), indicating that circRNAs from
405 unexplained stillbirth placentae are more susceptible to RNase H1 degradation, likely
406 indicating a deficiency of endogenous RNase H1 in these samples.

407

408 **3.05 Telomere length is decreased in stillbirth compared with healthy term**
409 **placenta tissue**

410 Relative telomere lengths (**Figure 2A**) were significantly reduced by ~40% in stillbirth
411 (3.108±1.954) compared with healthy placentae from 37 weeks' (5.881±2.823; $p < 0.05$). There
412 were no other significant differences in relative telomere lengths between 37, 38
413 (5.321±2.390), 39 (5.119±2.943), 40 (4.794±2.510), 41+ (4.564±2.428) weeks' gestation, and
414 stillbirth.

415

416 **3.06 Expression of senescence-associated genes is increased in aged healthy and**
417 **stillbirth placenta tissue**

418 Saul *et al.*[29] validated a gene set which identifies senescent cells and predicts senescence-
419 associated pathways in tissue. mRNA expression of senescence-associated genes (**Figure 2B**)
420 was significantly increased in 41+ weeks' gestation healthy placentae (all $p<0.0001$) and
421 stillbirth placentae ($p_{CXCL8}<0.0001$; $p_{CST3}<0.0001$; $p_{TYROBP}=0.0003$; $p_{FCER1G}<0.0001$;
422 $p_{LYZ}<0.0001$; $p_{CCL3}<0.0001$; $p_{CTSS}<0.0001$; $p_{AIF1}<0.0001$; $p_{HMGA1}<0.0001$; $p_{HIRA}<0.0001$)
423 compared with 37 weeks' gestation healthy placentae.

424 mRNA expression of *TYROBP* only was significantly increased in 41+ weeks' gestation
425 healthy placentae compared with stillbirth placentae ($p = 0.0038$).

426

427 **3.07 DNA damage is increased in aged healthy and stillbirth placenta tissue**

428 DNA damage was assessed using the Comet Assay that yields a Tail DNA% metric, an
429 indication of the level of DNA damage in placental cells. Representative images of healthy
430 cells (**Figure 2C**) and DNA damaged cells (**Figure 2D**) are included for reference. Tail DNA
431 % was significantly higher in cells from placentae sampled at 40 compared with 37 and 38
432 weeks' gestation (p_{37}=0.0381, p_{38}=0.0203; **Figure 2E**), and 41+ compared with 37, 38, 39 and
433 40 weeks' gestation (all p<0.0001) as well as in placentae from stillbirths compared with 37,
434 38, 39 and 40 weeks' gestation (p_{37}<0.0001, p_{38}<0.0001, p_{39}<0.0001, p_{40}=0.0001).

435

436 **3.08 circ_0000284 is primarily expressed in syncytiotrophoblasts**

437 Patient-derived TSCs (**Figure 3A**) were isolated and underwent cellular reprogramming to
438 either syncytiotrophoblasts (**Figure 3B**) or extravillous trophoblasts (**Figure 3D**). qPCR
439 detected circ_0000284 in syncytiotrophoblasts (**Figure 3C**), where abundance increased with
440 each passage (mean P1=0.045, P2=0.064, P3=0.098, P4=0.120), but was not detected in
441 extravillous trophoblasts (**Figure 3E**).

442

443 **3.09 *In vitro* knockdown of circ_0000284**

444 Hallmarks of cellular ageing include cellular senescence and DNA damage[30]. circR-loops
445 introduce steric hinderance with the formation of the circRNA:DNA hybrid, which can
446 promote transcriptional pausing and subsequent DNA breaks[31-33], resulting in genomic
447 instability[34]. As such, we investigated whether circ_0000284 induces cellular senescence and
448 DNA damage. This was confirmed using a custom-designed circ_0000284-specific siRNA in
449 patient-derived TSCs, reprogrammed to syncytiotrophoblasts.

450

451 *Validation of the siRNA knockdown*

452 Cultured primary syncytiotrophoblasts were either untreated (control), treated with a scrambled
453 siRNA or with a custom-designed siRNA specific to circ_0000284. Cells were then cultured
454 for 72 hours prior to harvesting for qPCR analyses as well as Comet Assay.

455

456 As shown in **Figure 3F**, transfection with the scrambled siRNA did not alter the expression of
457 the linear *HIPK3* mRNA (shown as abundance relative to *YWHAZ* and *ACTB*) compared to
458 control. Importantly, administration of the siRNA specific to circ_0000284 did not alter the
459 expression of linear *HIPK3* mRNA. However, the siRNA successfully reduced the relative
460 abundance of circ_0000284 compared with both the untreated cells (control) and cells treated
461 with the scrambled siRNA (all $p<0.0001$).

462

463 DRIP-qPCR confirmed that circ_0000284 forms a circR-loop in primary syncytiotrophoblasts
464 (mean 0.148%; $p<0.0001$ compared with RNase H-treated control; **Figure 3G**) and
465 administration of the siRNA specific to circ_0000284 significantly reduced circR-loop
466 formation (mean 0.029%; $p<0.0001$).

467

468 3.10 Expression of senescence-associated genes is attenuated with depletion of 469 circ_0000284

470 mRNA expression of senescence-associated genes (**Figure 3H**) was significantly decreased in
471 cells transfected with the siRNA specific to circ_0000284 compared to control; *CXCL8*
472 ($p=0.0053$), *CCL3* ($p=0.0291$), *CTSS* ($p<0.0001$), *AIF1* ($p<0.0001$), *HMGA1* ($p<0.0001$) and
473 *HIRA* ($p=0.0005$). mRNA expression of *CST3*, *TYROBP*, *FCER1G* and *LYZ* was not
474 significantly changed.

475

476 **3.11 DNA damage is mitigated with depletion of circ_0000284**

477 Transfection with the siRNA specific to circ_0000284 in primary syncytiotrophoblasts
478 significantly reduced the level of DNA damage (tail DNA%; **Figure 3I**) compared with both
479 the control (reduced by 41.3%) and scrambled (reduced by 39.5%) groups (all $p<0.0001$).
480 Transfection with the scrambled siRNA did not alter the level of DNA damage (tail DNA%)
481 compared with the control, indicating that depletion of circ_0000284 results in reduced DNA
482 damage.

483

484 **3.12 circRNAs can be detected in blood as a proxy measurement of placental**
485 **ageing**

486 Candidate circRNAs hsa_circ_0009000 (p=0.0137), hsa_circ_0036877 (p=0.0002),
487 hsa_circ_011277 (p=0.0052) and hsa_circ_0054624 (p=0.0158) were significantly more
488 abundant (**Figure 4**) in maternal blood sampled at 15-16 weeks' gestation in women who went
489 on to have a stillbirth compared with women who delivered live babies. Abundance of
490 hsa_circ_0024157, hsa_circ_0061017 and hsa_circ_0000284 were not significantly changed
491 between groups.

492 # 4. Comment

493 ## Principal Findings

494 Here, we confirm that placentae from stillbirth experience accelerated ageing (as determined
495 by typical hallmarks of decreased telomere length, increased rates of cellular senescence and
496 DNA damage). circRNAs circ_0009000, circ_0024157, circ_0061017, circ_0036877,
497 circ_0054624, circ_0111277 and circ_0000284 accumulate in ageing placental tissue, and
498 prematurely accumulate in stillbirth placentae. These circRNAs bind placenta DNA,
499 facilitating DNA breaks and cellular senescence. Measurement of candidate circRNAs in
500 maternal blood sampled at 15-16 weeks' gestation is a potential screening tool to indicate
501 premature placental ageing indicative of stillbirth risk.

502 ## Results in the Context of What is Known

503 *The accumulation of circRNAs*

504 The accumulation of circRNAs in aged tissue is a relatively recent discovery, evident from
505 studies[35] using *Drosophila melanogaster* photoreceptor neurons[36], mouse brain and heart[8] and
506 *Caenorhabditis elegans*[7]. It is likely that circRNAs accumulate in tissues as their lack of a 5'
507 cap and polyadenylated tail renders them resistant to exoribonuclease degradation[37]. Another
508 explanation for circRNA accumulation in some tissues is that in cell types such as neurons,
509 rates of mitosis and proliferation are lower than other cell types, allowing reduced turnover of
510 circRNAs[35,38-40]. Given that the nuclei of the syncytiotrophoblast are non-mitotic[41],
511 transcription is significantly reduced[42] and the syncytiotrophoblast displays markers of
512 senescence[43,44], this could be a primary area of circRNA accumulation. Indeed, this is

513 consistent with our *in vitro* findings of circRNAs expression primarily in the
514 syncytiotrophoblast.

515 Recently, circRNAs were identified as a potential forensic tool for estimating biological age in
516 human blood[45], which is an exciting leap from circRNA accumulation in animals to differential
517 circRNA expression with age in humans. Other studies have shown differentially expressed
518 circRNAs in human granulosa cells from women who were young versus those of advanced
519 reproductive age[46], and that specific circRNAs in human peripheral blood were associated with
520 parental longevity and cellular senescence[47]. The link between circRNA differential expression
521 and Alzheimer's disease is becoming more widely investigated[48], which is of particular interest
522 to this study given that Alzheimer's disease is, at its core, an ageing disorder[49]. Whilst these
523 studies demonstrate that expression of circRNAs is *changed* between differently aged groups,
524 none of these studies investigated circRNAs *accumulation* in ageing tissue.
525
526 We posit that the abundance of a circRNA is a combination of expression level as well as
527 accumulation. circRNA expression level can be increased by overexpressing the linear gene,
528 or by alternative splicing that promotes the circular over the linear transcript(s). circRNA
529 accumulation indicates that the circRNA remains in the tissue[35], unaffected by
530 exoribonucleases[37]. Over time, the abundance of the circRNA in the tissue increases as the
531 accumulated transcripts escape degradation. This occurs without change in the linear gene
532 expression nor alternative splicing. The result is that these circRNAs can continually exert their
533 function in the tissue well after their linear gene's expression and at higher-than-expected
534 abundance.
535

536

537 *Implications of circRNA accumulation as a novel mechanism for placental ageing*

538 Like other tissues in the body, the placenta undergoes the normal phenomenon of ageing.
539 Tissue ageing includes progressive increases in cellular senescence[50]. For the placenta, this
540 implies a decline in functionality as gestational age increases, resulting in a reduced capacity
541 of the placenta to support the fetus[3]. Placentae from stillbirths undergo an accelerated ageing
542 process[3], exhibiting similar pathological features regardless of their earlier gestational ages.
543 Markers of ageing such as increased DNA and RNA oxidation, lipid peroxidation, altered
544 perinuclear location of lysosomes and larger autophagosomes are found in placentae from
545 stillbirths as well as those from healthy late term compared with placentae from healthy early
546 term[3]. This study expands on the current literature, demonstrating shorter telomeres, increased
547 cellular senescence and DNA breaks occur with placental ageing.

548 A circR-loop is formed when a circRNA molecule binds one strand of helicase-unwound
549 genomic DNA[10]. The steric hindrance of this bulky structure causes RNA polymerase II to stall
550 during transcription, resulting in a DNA break, and often a subsequent fusion at another locus[51],
551 promoting genomic instability[11]. Double-stranded DNA breaks are lethal to cells, as they affect
552 both strands of DNA and promote the loss of genetic information[13]. Any type of DNA damage
553 can trigger cellular apoptosis or senescence[12]. Given that we observed increased DNA breaks
554 in stillbirth placentae, which also had elevated abundance of circ_0000284 binding to placental
555 DNA, we further determined that circ_0000284 induces DNA damage and cellular senescence
556 *in vitro*. Moreover, RNase H1 was investigated as a proposed method of circRNA degradation.
557 Knockdown of RNase H1 using siRNA revealed that a portion of all circRNAs are susceptible
558 to RNase H1 degradation in placenta tissue, however this was more impactful in placentae from
559 unexplained stillbirth. This could be due to a greater proportion of circRNAs susceptible to
560 RNase H1 in tissue, compared to circRNAs that are not susceptible, or could indicate a lack of

561 endogenous H1 in placentae from unexplained stillbirth. This would also potentially account
562 for the premature circRNA accumulation in these samples. Together, this presents a promising
563 avenue for investigation as a mechanism for stillbirth via premature placental ageing. This
564 study also provides evidence that circRNAs accumulate in healthy ageing placental tissue, and
565 can also be detected as a novel proxy measure of placental ageing in maternal blood.

566

567 **Clinical Implications**

568 Our group 41+ weeks' gestation encompassed women who birthed between 41+1 and 41+6
569 weeks'. Given that gestation of >40 weeks, in addition to maternal age ≥35 years[3] and male
570 fetal sex[1], are risk factors for stillbirth, the current Pregnancy Care Guidelines consider 42
571 weeks' and beyond as post-term and recommend fetal monitoring and induction of labour from
572 41 weeks', even in uncomplicated, low risk patients[52]. Indeed, evidence shows that stillbirth
573 and neonatal death can be reduced with fetal surveillance twice weekly from 39 weeks'[53].

574 In this study, placentae from stillbirths displayed evidence of further ageing hallmarks. As these
575 stillbirth placentae were collected at gestational weeks 23, 26, 31 and 34, this clearly indicates
576 that in stillbirth the placenta experiences accelerated tissue ageing, resulting in a post-term
577 phenotype much earlier than would be appropriate for their gestational age. Use of a blood test
578 for signalling accelerated placental ageing, as supported by our results, could be beneficial to
579 screen for pregnancies at high risk of stillbirth.

580

581 **Research Implications**

582 Interpreting our results, we propose the following mechanism as a potential contributor to
583 stillbirth pathology (**Figure 5**): In uncomplicated pregnancy, circRNAs naturally accumulate
584 in placental cells as the tissue ages with gestation. However, in pregnancies resulting in
585 unexplained stillbirth, premature placental ageing results in accelerated accumulation of
586 circRNAs. These circRNAs form circR-loops, with at least one circRNA (circ_0000284)
587 known to facilitate DNA damage and induce senescence. As DNA breaks facilitate genomic
588 instability[11] and cellular senescence[54] and apoptosis[55], this may result in reducing placental
589 function to the detriment of the fetus.

590

591 **Strengths and Limitations**

592 We confirm that circRNAs accumulate in human aged tissue. Importantly, we established that
593 there is no global increase in total RNA, nor circular RNA, abundance with placental
594 gestational age; hence, our candidate circRNAs are unique in their ability to accumulate with
595 age. It should be noted that accumulation of these specific circRNAs with age may be placenta-
596 specific, as this study only examined placental tissue, and this candidate list may not be
597 exhaustive. Further studies will profile all accumulating circRNAs in the placenta as it ages.

598

599 Additionally, this study is limited by the small sample size of stillbirth placentae; however, this
600 is a common issue in stillbirth research[3,56] given the difficulty in obtaining tissue within an
601 appropriate timeframe. As stillbirths that could be explained by fetal congenital abnormality
602 were excluded, resulting in a pure "unexplained stillbirth" sample pool, this further reduced
603 available tissue samples. Moreover, sample size limited our ability to perform fetal sex-specific

604 statistical tests. Further studies will be conducted with larger sample sizes to allow for increased
605 comparisons. Future studies will also include participants of different ethnicities, accounting
606 for ethnicities which are more prone to stillbirths (such as South Asian women[53]).

607

608 **Conclusions**

609 circRNAs accumulate in ageing human placental tissue, in the absence of any change in total
610 linear or circular RNA expression nor alternative splicing variants. Importantly, circRNAs
611 circ_0009000, circ_0024157, circ_0061017, circ_0036877, circ_0054624, circ_0111277 and
612 circ_0000284 are present at exceptionally high levels in placenta from stillbirths, similar to or
613 surpassing the circRNA levels found in post-term placentae. We provide evidence that these
614 circRNAs bind to DNA to form circR-loops in placental tissue. *In vitro* experiments in primary
615 human syncytiotrophoblasts show that knockdown of circ_000284 results in decreased DNA
616 breaks in cells, indicating that this circRNA facilitates DNA damage, and decreased expression
617 of senescence-associated genes, implying that this circRNA induces cellular senescence.
618 Finally, measurement of candidate circRNAs in maternal blood sampled at 15-16 weeks'
619 gestation is a viable tool to screen for accelerated placental ageing, as a proxy for risk of
620 stillbirth.

621

Acknowledgments

We thank the women who consented to their placental tissue being used for this research. Thank you to the clinical and anatomical staff from the Women's and Children's Hospital and Lyell McEwin Hospital who were involved in the women's care, and who collected and biopsied the placental samples. Thank you to Professor Jose Polo for his insightful suggestions. Figures were created using Biorender.com

Author Contributions

A.L.A. conceptualised this work, performed experimental work and formal analysis of data, original draft preparation, and review and editing. M.R.J., H.S.S. and C.P.B. provided stillbirth placenta samples and reviewed and edited the manuscript. D.M. contributed to experimental work and data analysis. S.W. provided molecular expertise and reviewed and edited the manuscript. M.D.S. and T.J-K. reviewed and edited the manuscript. G.A.D. provided clinical expertise and reviewed and edited the manuscript. C.T.R. provided supervision, funding acquisition, interpretation of data, review and editing of the manuscript. All authors contributed to the article and approved the final version.

Funding

A.L.A. is supported by funding from the Flinders Foundation, Flinders University, the Channel 7 Children's Research Foundation and a Future Making Fellowship from the University of Adelaide.

C.T.R. is supported by an NHMRC Investigator Grant (GNT1174971) and a Matthew Flinders Fellowship from Flinders University.

The Genomic Autopsy Study was supported by NHMRC (#APP1123341), Genomics Health Futures Mission – Medical Research Futures Fund (#GHFM76777) and the Australian Genomic Health Alliance NHMRC Targeted Call for Research into Preparing Australia for the Genomics Revolution in Healthcare (#GNT1113531) to H.S.S. and C.P.B.

References

1 (ed Australian Institute of Health and Welfare) (Australian Institute of Health and Welfare, 2018).

2 Hug, L. *et al.* Global, regional, and national estimates and trends in stillbirths from 2000 to 2019: a systematic assessment. *The Lancet* **398**, 772-785 (2021).

3 Maiti, K. *et al.* Evidence that fetal death is associated with placental aging. *Am J Obstet Gynecol* **217**, 441 (2017).

4 Ferrari F, F. F., Saade G, Menon R. Placental telomere shortening in stillbirth: a sign of premature senescence? *Journal of Maternal-Fetal and Neonatal Medicine* **29**, 1283-1288 (2016). https://doi.org/DOI: 10.3109/14767058.2015.1046045

5 Amir, H. *et al.* A piece in the puzzle of intrauterine fetal death: pathological findings in placentas from term and preterm intrauterine fetal death pregnancies. *The journal of maternal-fetal & neonatal medicine* **22**, 759-764 (2009).

6 Westholm, J. O. *et al.* Genome-wide analysis of drosophila circular RNAs reveals their structural and sequence properties and age-dependent neural accumulation. *Cell reports* **9**, 1966-1980 (2014).

7 Cortes-Lopez M, G. M., Cooper DA, Gruner HN, Voda AI, van der Linden AM, Miura P. Global accumulation of circRNAs during aging in Caenorhabditis elegans. *BMC Genomics* **19** (2018).

8 Gruner H, C.-L. M., Cooper DA, Bauer M, Miura P. . CircRNA accumulation in the aging mouse brain. *Sci Rep* **6**, 38907 (2016).

9 Arthurs, A. L., Jankovic-Karasoulos, T., Smith, M. D. & Roberts, C. T. Circular RNAs in Pregnancy and the Placenta. *International Journal of Molecular Sciences* **23**, 4551 (2022).

10 Conn, S. J. *et al.* The RNA binding protein quaking regulates formation of circRNAs. *Cell* **160**, 1125-1134 (2015).

11 Lord, C. J. & Ashworth, A. The DNA damage response and cancer therapy. *Nature* **481**, 287-294 (2012).

12 Parrinello, S., Coppe, J.-P., Krtolica, A. & Campisi, J. Stromal-epithelial interactions in aging and cancer: senescent fibroblasts alter epithelial cell differentiation. *Journal of cell science* **118**, 485-496 (2005).

13 Altaf, M., Saksouk, N. & Côté, J. Histone modifications in response to DNA damage. *Mutation Research/Fundamental and Molecular Mechanisms of Mutagenesis* **618**, 81-90 (2007).

14 Ren, L. *et al.* Mechanisms of circular RNA degradation. *Communications Biology* **5**, 1355 (2022).

15 Li, X. *et al.* Linking circular intronic RNA degradation and function in transcription by RNase H1. *Science China Life Sciences* **64**, 1795-1809 (2021).

16 Mohammed, H. *et al.* Safety and protective effects of maternal influenza vaccination on pregnancy and birth outcomes: A prospective cohort study. *EClinicalMedicine* **26**, 100522 (2020).

17 Byrne, A. B. *et al.* Genomic autopsy to identify underlying causes of pregnancy loss and perinatal death. *Nature Medicine* **29**, 180-189 (2023).

18 Arthurs, A. L. *et al.* Genetically edited human placental organoids cast new light on the role of ACE2. *Cell Death & Disease* **16**, 78 (2025). https://doi.org/10.1038/s41419-025-07400-x

19 Dietrich, B. *et al.* NOTCH3 signalling controls human trophoblast stem cell expansion and differentiation. *Development* **150**, dev202152 (2023).

20 Haider, S. *et al.* Self-renewing trophoblast organoids recapitulate the developmental program of the early human placenta. *Stem cell reports* **11**, 537-551 (2018).

21 Tan, J. P., Liu, X. & Polo, J. M. Establishment of human induced trophoblast stem cells via reprogramming of fibroblasts. *Nature protocols* **17**, 2739-2759 (2022).

22 Vilades, D. *et al.* Plasma circular RNA hsa_circ_0001445 and coronary artery disease: Performance as a biomarker. *The FASEB Journal* **34**, 4403-4414 (2020).

23 Drula, R., Braicu, C., Chira, S. & Berindan-Neagoe, I. Investigating circular RNAs using qRT-PCR; roundup of optimization and processing steps. *International Journal of Molecular Sciences* **24**, 5721 (2023).

24 Wu, H. *et al.* Determination of the role of the human RNase H1 in the pharmacology of DNA-like antisense drugs. *Journal of Biological Chemistry* **279**, 17181-17189 (2004).

25 Livak, K. J. & Schmittgen, T. D. Analysis of relative gene expression data using real-time quantitative PCR and the 2− ΔΔCT method. *methods* **25**, 402-408 (2001).

26 Cawthon, R. M. Telomere length measurement by a novel monochrome multiplex quantitative PCR method. *Nucleic acids research* **37**, e21-e21 (2009).

27 Sanz, L. A. & Chédin, F. High-resolution, strand-specific R-loop mapping via S9. 6-based DNA–RNA immunoprecipitation and high-throughput sequencing. *Nature protocols* **14**, 1734-1755 (2019).

28 Morosin, S. K. *et al.* The (pro) renin receptor and soluble (pro) renin receptor in choriocarcinoma. *Reproduction* **162**, 375-384 (2021).

29 Saul, D. *et al.* A new gene set identifies senescent cells and predicts senescence-associated pathways across tissues. *Nature communications* **13**, 4827 (2022).

30 Qi, H., Xiong, L. & Tong, C. Aging of the placenta. *Aging (Albany NY)* **14**, 5294 (2022).

31 El Hage, A., Webb, S., Kerr, A. & Tollervey, D. Genome-wide distribution of RNA-DNA hybrids identifies RNase H targets in tRNA genes, retrotransposons and mitochondria. *PLoS genetics* **10**, e1004716 (2014).

32 Alexander, R. D., Innocente, S. A., Barrass, J. D. & Beggs, J. D. Splicing-dependent RNA polymerase pausing in yeast. *Molecular cell* **40**, 582-593 (2010).

33 Wongsurawat, T., Jenjaroenpun, P., Kwoh, C. K. & Kuznetsov, V. Quantitative model of R-loop forming structures reveals a novel level of RNA–DNA interactome complexity. *Nucleic acids research* **40**, e16-e16 (2012).

34 Conn, V. M. *et al.* Circular RNAs drive oncogenic chromosomal translocations within the MLL recombinome in leukemia. *Cancer cell* **41**, 1309-1326. e1310 (2023).

35 Knupp, D. & Miura, P. CircRNA accumulation: A new hallmark of aging? *Mech Ageing Dev* **173**, 71-79 (2018). https://doi.org/doi:10.1016/j.mad.2018.05.001

36 Hall H, M. P., Cooper DA. et al. . Transcriptome profiling of aging Drosophila photoreceptors reveals gene expression trends that correlate with visual senescence. *BMC Genomics* **18** (2017). https://doi.org/https://doi.org/10.1186/s12864-017-4304-3

37 Jeck, W. *et al.* Circular RNAs are abundant, conserved, and associated with ALU repeats. *RNA* **19**, 141-157 (2013). https://doi.org/doi:10.1261/rna.035667.112.

38 Rybak-Wolf, A. *et al.* Circular RNAs in the mammalian brain are highly abundant, conserved, and dynamically expressed. *Molecular cell* **58**, 870-885 (2015).

39 Bachmayr-Heyda, A. *et al.* Correlation of circular RNA abundance with proliferation–exemplified with colorectal and ovarian cancer, idiopathic lung fibrosis and normal human tissues. *Scientific reports* **5**, 8057 (2015).

40 Song, X. *et al.* Circular RNA profile in gliomas revealed by identification tool UROBORUS. *Nucleic acids research* **44**, e87-e87 (2016).

41 Mayhew, T. & Simpson, R. Quantitative evidence for the spatial dispersal of trophoblast nucleic in human placental villi during gestation. *Placenta* **15**, 837-844 (1994).

42 Huppertz, B., Frank, H.-G., Reister, F., Korr, H. & Kaufmann, P. Apoptosis cascade progresses during turnover of human trophoblast: analysis of villous cytotrophoblast and syncytial fragments in vitro. *Laboratory investigation; a journal of technical methods and pathology* **79**, 1687-1702 (1999).

43 Chuprin, A. *et al.* Cell fusion induced by ERVWE1 or measles virus causes cellular senescence. *Genes & development* **27**, 2356-2366 (2013).

44 Goldman-Wohl, D. & Yagel, S. United we stand not dividing: the syncytiotrophoblast and cell senescence. *Placenta* **35**, 341-344 (2014).

45 Wang, J. *et al.* Circular RNA as a potential biomarker for forensic age prediction. *Frontiers in Genetics* **13**, 29 (2022).

46 Cheng, J. *et al.* Circular RNA expression profiling of human granulosa cells during maternal aging reveals novel transcripts associated with assisted reproductive technology outcomes. *PLoS ONE* **12**, e0177888 (2017). https://doi.org/https://doi.org/10.1371/journal.pone.0177888

47 Haque, S. *et al.* circRNAs expressed in human peripheral blood are associated with human aging phenotypes, cellular senescence and mouse lifespan. *GeroScience* **42**, 183-199 (2020). https://doi.org/10.1007/s11357-019-00120-z

48 Akhter, R. in *Circular RNAs* (ed J Xiao) (Springer Nature, 2018).

49 Smith, M. A., Sayre, L. M., Monnier, V. M. & Perry, G. Radical AGEing in Alzheimer's disease. *Trends in neurosciences* **18**, 172-176 (1995).

50 Holt, D., Grainger, DW. Senescence and quiescence induced compromised function in cultured macrophages. *Biomaterials* **33**, 7497-7507 (2012).

51 Conn, V. M. *et al.* A circRNA from SEPALLATA3 regulates splicing of its cognate mRNA through R-loop formation. *Nature Plants* (2017).

52 Australian_Government_Department_of_Health. (ed Department of Health) (Canberra, 2020).

53 Davies-Tuck, M. L., Davey, M.-A., Hodges, R. L. & Wallace, E. M. Fetal surveillance from 39 weeks' gestation to reduce stillbirth in South Asian-born women. *American Journal of Obstetrics and Gynecology* **229**, 286. e281-286. e289 (2023).

54 McHugh, D. & Gil, J. Senescence and aging: Causes, consequences, and therapeutic avenues. *Journal of Cell Biology* **217**, 65-77 (2018).

55 Baar, M. P. *et al.* Targeted apoptosis of senescent cells restores tissue homeostasis in response to chemotoxicity and aging. *Cell* **169**, 132-147. e116 (2017).

56 Hannan, N. J. *et al.* Circulating mRNAs are differentially expressed in pregnancies with severe placental insufficiency and at high risk of stillbirth. *BMC Medicine* **18**, 145 (2020). https://doi.org/10.1186/s12916-020-01605-x

785 ***Table 1.*** *Materials required for preparation of TSC, syncytiotrophoblast and extravillous*
786 *trophoblast differentiation media.*

	Concentration	**Manufacturer**
TSC media		
DMEM/F12 GlutaMAX	Base media	Gibco
B-27	1x	Gibco
Insulin-Transferrin-Selenium-Ethanolamine (ITS-X)	1x	Gibco
A83-01	1 µM	Tocris
Recombinant human epidermal growth factor (rhEGF)	50 ng/mL	R&D Systems
CHIR99021	2 µM	Tocris
Y27632	5 µM	Santa Cruz
Syncytiotrophoblast differentiation media		
DMEM/F12 GlutaMAX	Base media	Gibco
Bovine serum albumin (BSA)	0.3% (wt/vol)	Sigma-Aldrich
Insulin-Transferrin-Selenium-Ethanolamine (ITS-X)	1x	Gibco
A83-01	7.5 µM	Tocris
2-mercaptoethanol	0.1 mM	Sigma-Aldrich
Y27632	2.5 µM	Santa Cruz
KnockOut serum replacement (KSR)	4% (vol/vol)	Thermo Fisher
Forskolin	2 µM	Sigma-Aldrich
Extravillous trophoblast differentiation media		
DMEM/F12 GlutaMAX	Base media	Gibco
Bovine serum albumin (BSA)	0.3% (wt/vol)	Sigma-Aldrich
Insulin-Transferrin-Selenium-Ethanolamine (ITS-X)	1x	Gibco
A83-01	7.5 µM	Tocris
2-mercaptoethanol	0.1 mM	Sigma-Aldrich
Y27632	2.5 µM	Santa Cruz
KnockOut serum replacement (KSR)	4% (vol/vol)	Thermo Fisher
hNRG1-β1 *NB! Add to media only for first 6 days of culture, then remove	100 ng/mL	Cell Signalling Technology

787

Table 2. *Primer sequences and melt temperatures (T_m) used for qPCR*

Gene	Transcript	Forward primer	Reverse primer	T_m
CRHR2	XM_024446665.1	ATGGACGCGGCACTGCT	ACTGCAGCCTGGCGCT	57
	XM_017011752.2	TCCTACTGCAACACGACCTT	GTTGATCTTTGAGGCCCACG	59
	NM_001202483.2	AGAAAGAGATGTGTGCCAAGC	CCAGAGGAAGAAGGTGGAGG	58
	NM_001202482.2	CTCACTCTCGCGTCCACTC	GTTGATCTTTGAGGCCCACG	59
	NM_001202481.1	GGTCAAATGGGAAGAGAGCC	GTGTTGTACTTGACGCCGTT	58
	NM_001202475.1	CATGACCCTCACCAACCTCT	AAGGTCGTGTTGCAGTAGGA	58
	Circular: circ_0009000	TGGCTACAATTCCTGCTCCA	ACATCTGCTGCTTTGTGTGG	59
CWF19L2	XM_017017239.2	AGATGGTGGATTAAGCTGGCT	GAATGGACTCACGCTCTGGA	59
	XR_947795.2	CCAGAAAGGGAGTATGAACAAAC	CCATGTCACCCACTTCCTTG	57
	NM_152434.3	AGCCATCGGAAACCAGTACT	CCATGTCACCCACTTCCTTG	58
	XM_011542620.3	TCATGGAGTCGCTCTGATGG	ACATCAGGGAATGGGCTCTT	58
	Circular: circ_0024157	AGAAGTGATATACCATTCTTAAATGTA	GATAAATTACAAAATTACATGGATAA	53
RAB22A	NM_020673.3	TATTGTGTGGCGGTTTGTGG	TCTTGTCCAGCTGTATCCCA	58
	Circular: circ_0061017	CCCATTGGCTGAACTCTTCC	AGCCACTACACTTGTTCTTGA	57
FURIN	NM_001382622.1	GCATCATCGACATCCTCACC	GTCTCCACGTCATTCTCGGT	58
	NM_002569.4	ACATCCTCACCGAGCCCA	GACTCTCGGCTGCTCTGG	59
	NM_001382619.1	GTGCAGTCCTCCCTCGAC	TCACTCCTCGATGCCAGAAG	59
	NM_001289823.2	CGGTCGCCTGGAAAAGTT	CTGGACGATGGCATCGAGA	58

	NR_168464.1	(distinguished by product size)		
	NM_001382620.1	GACTCGGGTGCGGGATC	TGTTGCTGCTACCACCCATA	58
	NM_001382621.1	CCAAGAACACAGCCAGGAAG	TACCACCCATAGCAACCAGG	58
	NM_001289824.2	GGTTTGAGACAAACTGGGACTAG	GACCAAGGTTCCTGTTGCTG	58
	Circular: circ_0036877	TTTGTAAGATGCTGGGTTGGTG	ACTGCATCTGTCACCTCGC	57
PNPT1	NM_033109.5	CCTTCCCAGTTTATGCCTTTGG	AAAGAGCGGTCTAATTGAACGAT	60
	Circular: circ_0054624	AGCATGTTAGGCAATGTTGAT	TTTACTGACCGCTGTGACCA	60
PAPPA2	XM_005245422.3	GCATCTCAGCTGTGGCTCTA	AGTTACTGGGAGCCGAAAGAC	56
	Circular: circ_0111277	AGTCGATGGATTCCTCTCAT	AAGTTGTTCATCACTCTGTT	55
HIPK3	NM_001278163.2	GTCTTTGGGAGTTAAACCGACT	ACACAACTGCTTGGCTCTAC	59
	NM_001048200.3	GTTTCGCCGTTTCCTCTCAG (distinguished by product size)	ACTTCCTCGACATCTTTCCCA	60
	NM_005734.5			
	XM_047426224.1	GCAGTCCTAGGCCGTAACTA (distinguished by product size)	ACTTCCTCGACATCTTTCCCA	60
	XM_047426223.1			
	XM_047426225.1	ATGGAGCAGAGTCTTTGA	TTGCCGCTGTTTGTCTGAAA	59
	NM_001278162.2	AGGGAGACGGCTGTTGTAAA	ACACAACTGCTTGGCTCTAC	60
	Circular: circ_0000284	CTGTGTATTTTCAGTCTGGCCT	GATGGGTGGCAAATCAAAATGT	58
YWHAZ		ACCGTTACTTGGCTGAGGTTGC	CCCAGTCTGATAGGATGTGTTGG	60
GAPDH		TCAAGGCTGAGAACGGGAAG	CGCCCCACTTGATTTTGGAG	60
ACTINB		CACCATTGGCAATGAGCGGTTC	AGGTCTTTGCGGATGTCCACGT	60
CXCL8		AAGCTGGCCGTGGCTCTCTTG	AGCCCTCTTCAAAAACTTCTC	60
CST3		CAACAAAGCCAGCAACGACA	TCTTGGTACACGTGGTTCGG	60
TYROBP		ACTGAGACCGAGTCGCCTTAT	ATACGGCCTCTGTGTGTTGAG	61
FCER1G		AGCAGTGGTCTTGCTCTTACT	TGCCTTTCGCACTTGGATCTT	62

LYZ	CTTGTCCTCCTTTCTGTTACGG	CCCCTGTAGCCATCCATTCC	60
CCL3	TTCTCTGTACCATGACACTCTGC	CGTGGAATCTTCCGGCTGTAG	61
CTSS	CCATTGGGATCTCTGGAAGAAAA	TCATGCCCACTTGGTAGGTAT	59
AIF1	ATCAACAAGCAATTCCTCGATGA	CAGCATTCGCTTCAAGGACATA	60
HMGA1	GCTGGTAGGGAGTCAGAAGGA	TGGTGGTTTTCCGGGTCTTG	62
HIRA	TTCAGTTGATATTCACCCTGACG	AAGTGATTGTCCATCTGGCAAA	59

Table 3. *Characteristics of women and infants from the study by gestational age group (weeks ')*

	Gestational Age group (weeks')					Stillbirth
	37	**38**	**39**	**40**	**41+ †**	
Maternal age (years)	28.7 ± 1.5	24.1 ± 2.9	25.9 ± 1.9	28.3 ± 4.5	26.8 ± 4.2	#1: 35 #2: 26 #3: 33 #4: 28
Maternal BMI (kg/m^2)	26.4 ± 5.8	27.2 ± 9.1	23.1 ± 4.3	20.8 ± 4.1	23.4 ± 6.2	#1: DM #2: DM #3: DM #4: 22.8
Smoking status*	1/12	2/12	1/12	3/12	2/12	#1: DM #2: DM #3: DM #4: N
Gestational age (weeks)	37.1 ± 0.9	38.0 ± 0.3	39.1 ± 0.7	40.0 ± 0.4	41.5 ± 0.3	#1: 23 #2: 26 #3: 34 #4: 31
Birthweight (g)	2962 ± 325	3345 ± 465	3089 ± 201	3702 ± 161	3513 ± 277	#1: 256 #2: 800 #3: 2546 #4: 1140
Fetal sex^	XX = 6 XY = 6	XX = 6 XY = 6	XX = 7 XY = 5	XX = 6 XY = 6	XX = 6 XY = 6	#1: XX #2: XY #3: XY #4: XX

Data are presented as mean ± standard error of the mean.

DM = Data Missing, as data were not available at the time of sample collection.

* Smoking status as self-reported by patient at time of delivery. X/12 indicates the number of women who reported YES to smoking while pregnant out of the total 12 women. For stillbirths, Y = Yes, N = No.

^ Where XX = female, XY = male.

† The group "41+ weeks' gestation" is defined as delivery at 41+0 through to 41+6 weeks' gestation.

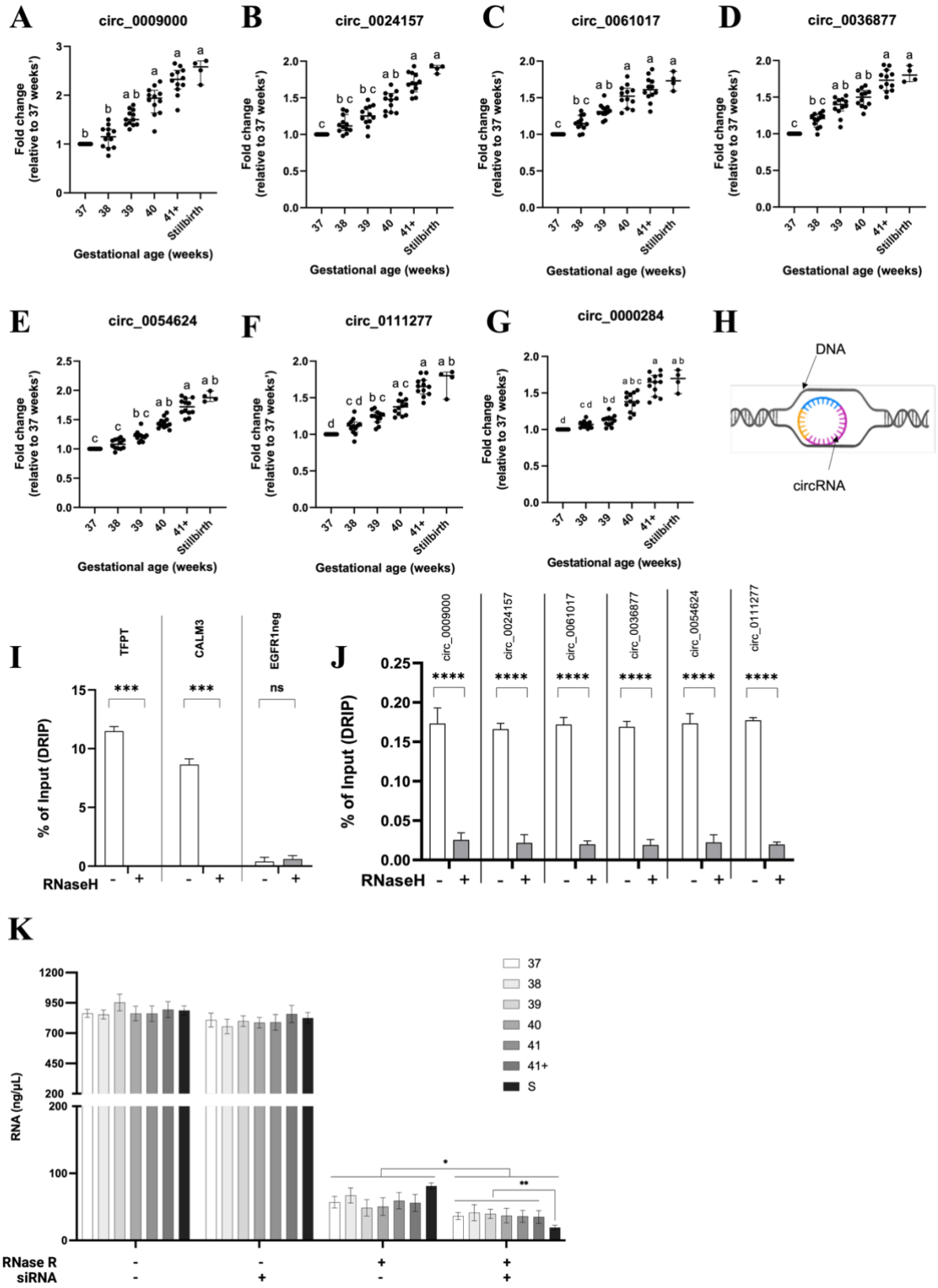
A
circ_0009000
B
circ_0024157
C
circ_0061017
D
circ_0036877
E
circ_0054624
F
circ_0111277
G
circ_0000284
Fold change (relative to 37 weeks')
Gestational age (weeks)
37
38
39
40
41+
Stillbirth
H
DNA
circRNA
I
TFPT
CALM3
EGFR1neg
% of Input (DRIP)
RNaseH
J
circ_0009000
circ_0024157
circ_0061017
circ_0036877
circ_0054624
circ_0111277
% of Input (DRIP)
RNaseH

K
RNA (ng/µL)
37
38
39
40
41
41+
S
RNase R
siRNA

Figure 1. *Abundance (as fold change relative to abundance at 37 weeks' gestation) of* ***(A)*** *circ_0009000,* ***(B)*** *circ_0024157,* ***(C)*** *circ_0061017,* ***(D)*** *circ_0036877,* ***(E)*** *circ_0054624,* ***(F)*** *circ_0111277 and* ***(G)*** *circ_0000284, in isolated cells from 37, 38, 39, 40 and 41+ uncomplicated, and stillbirth, placentae. n=12 placentae / uncomplicated gestational group, n=4 stillbirth placentae. Data are presented as scatter plots with bars, and indicate mean ± standard error of the mean.* ***(H)*** *Diagram of circR-loop, where the circRNA molecule binds to one strand of helically-unwound DNA. DRIP-qPCR analysis using primers for* ***(I)*** *R-loop-positive loci TFPT and CALM3, and R-loop-negative locus EGFR1neg, and* ***(J)*** *circ_0009000, circ_0024157, circ_0061017, circ_0036877, circ_0054624, circ_0111277 and circ_0000284. Where indicated, samples were treated with RNase H prior to DRIP. Treatment with RNase H significantly suppressed the DRIP-qPCR signal, consistent with R-loop formation in the tested regions. n=5 placentae with, and n=5 placentae without, RNase H treatment. DRIP-qPCR signal intensity shown as % of Input (DRIP), with indication of mean ± standard error of the mean.* ***(K)*** *Quantity of total RNA (ng / μL), starting with ~1μg total in isolated cells from 37, 38, 39, 40 and 41+ uncomplicated, and stillbirth, placentae. n=12 placentae / uncomplicated gestational group, n=4 stillbirth placentae. RNA quantified in the presence and absence of RNase R (degrades linear transcripts) and an siRNA specific for RNase H1 (enzyme which can degrade circRNAs). Different letters represent statistically significant ($p < 0.05$) differences. *** $p < 0.001$, **** $p < 0.0001$, ns = not significant.*

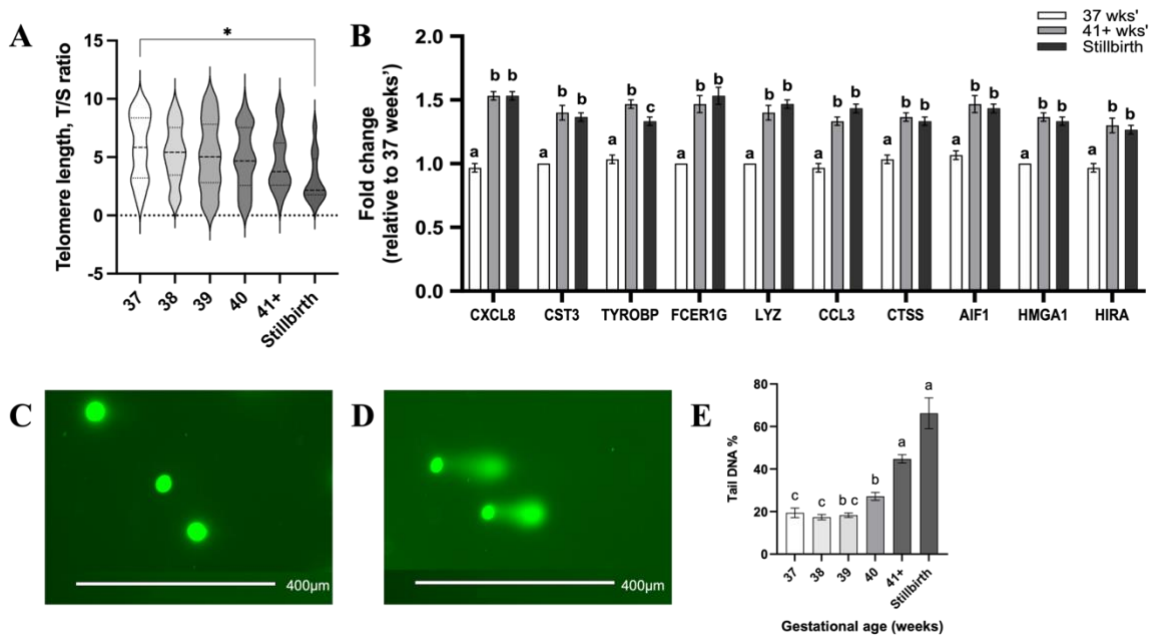

Figure 2. (A) *Telomere length (expressed as "T/S ratio", i.e. quantity of telomere DNA divided by quantity of a single copy gene), and* ***(B)*** *fold change mRNA expression of senescence-associated genes in placenta tissue from 37 weeks' gestation uncomplicated pregnancy (white), 41+ weeks' gestation uncomplicated pregnancy (grey) and stillbirth (black). Data are presented as (A) violin plots and (B) mean ± standard error of the mean. Representative images of* ***(C)*** *healthy cells and* ***(D)*** *DNA damaged cells, as imaged using epifluorescent microscopy after performing a Comet Assay.* ***(E)*** *Levels of DNA damage, as assessed by Tail DNA %, in isolated cells from 37, 38, 39, 40 and 41+ uncomplicated, and stillbirth, placentae. n=12 placentae / uncomplicated gestational group, n=4 stillbirth placentae. 100 cells analysed following Comet Assay, per placenta. Data are presented as mean ± standard error of the mean. Different letters represent statistically significant ($p < 0.05$) differences. * $p < 0.05$.*

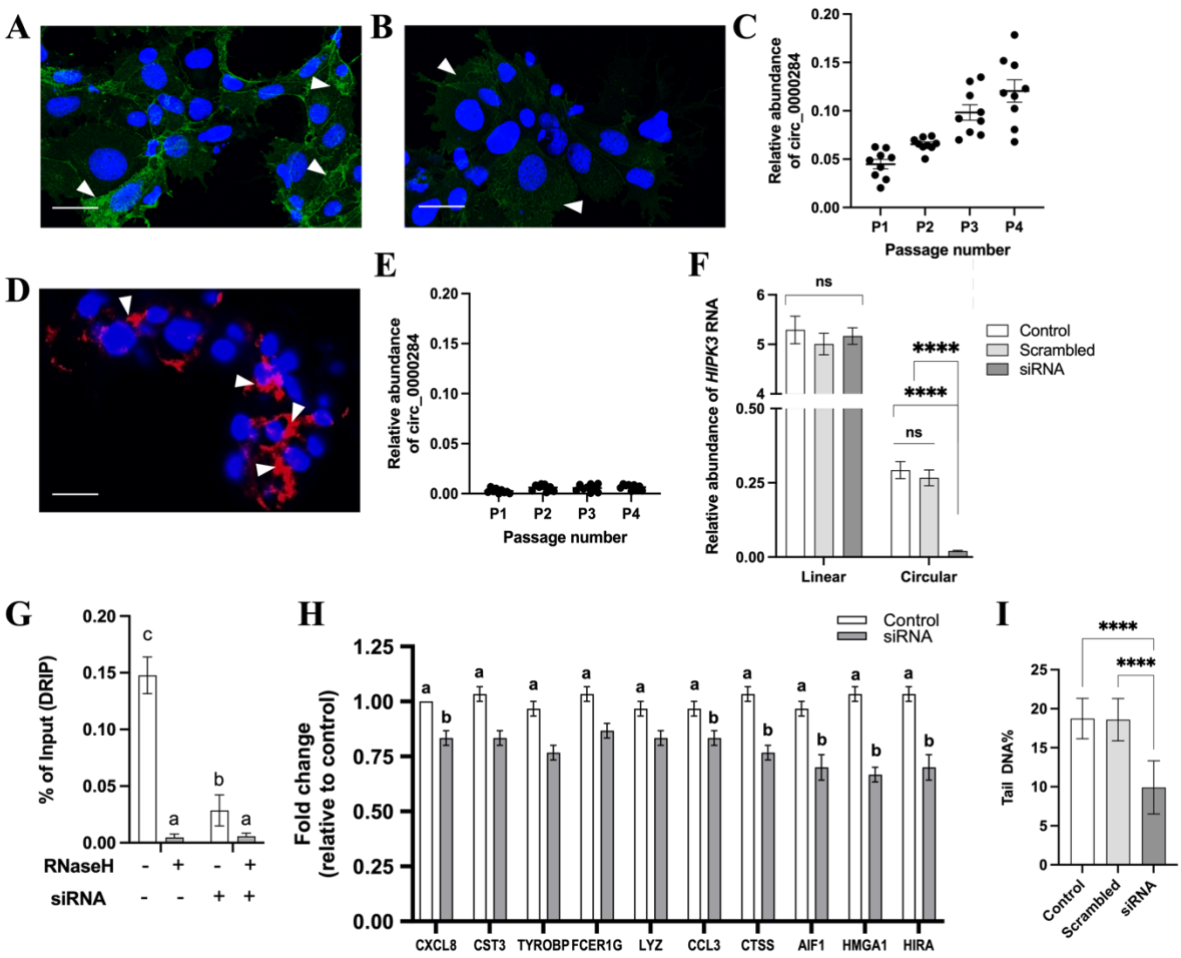

Figure 3. *Representative immunocytochemistry images of* ***(A)*** *not syncytialised TSCs,* ***(B)*** *syncytialised TSCs (i.e. reprogrammed to syncytiotrophoblasts) and* ***(D)*** *TSCs reprogrammed to extravillous trophoblasts. Scale bars: 10 µm. Nuclei are stained with DAPI (blue), green stain is for E-cadherin (cell membrane), red stain is for HLA-G (expressed in extravillous trophoblasts). White arrows indicate E-cadherin staining (A, B) and HLA-G staining (D). Relative abundance of circ_0000284 in cultured* ***(C)*** *syncytiotrophoblasts, and* ***(E)*** *extravillous trophoblasts, over four culture passages. Data are presented as scatter plots with bars, and indicate mean ± standard error of the mean.* ***(F)*** *Abundance of HIPK3 RNA ("linear") and circ_0000284 ("circular") in cultured syncytiotrophoblast cells, either untransfected ("control"), transfected with a scrambled siRNA ("scrambled") or transfected with an siRNA specific to circ_0000284 ("siRNA").* ***(G)*** *DRIP-qPCR using primers for circ_0000284, in syncytiotrophoblasts treated with combinations of RNase H and siRNA as indicated.* ***(H)*** *Fold change mRNA expression of senescence-associated genes in syncytiotrophoblasts, either untreated (white) or treated with siRNA (grey).* ***(I)*** *Levels of DNA damage, as assessed by Tail DNA %, in syncytiotrophoblast cells. n=5 patients / group. 100 cells analysed following Comet Assay, per sample. Data are presented as mean ± standard error of the mean. Different letters represent statistically significant ($p < 0.05$) differences. **** $p < 0.0001$, ns = not significant.*

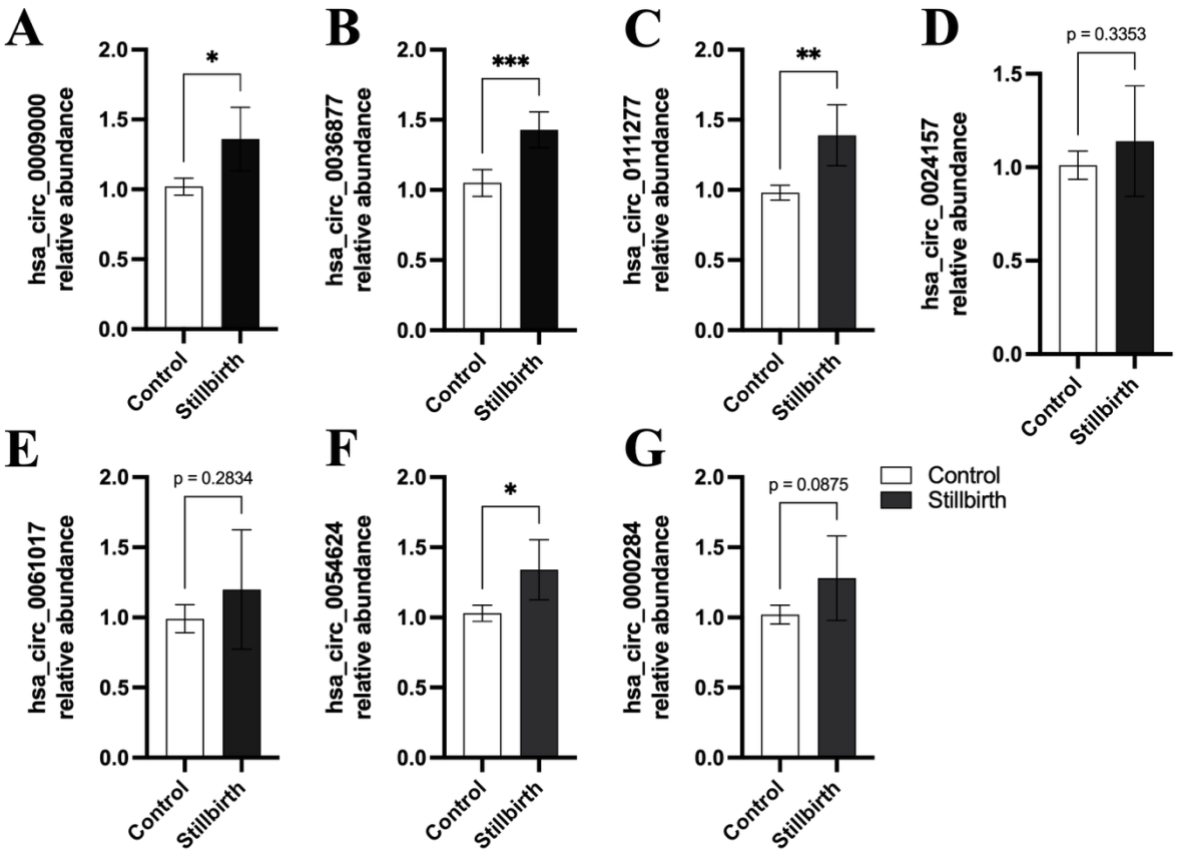

Figure 4. *Abundance (as fold change relative to housekeeping genes) of* ***(A)*** *hsa_circ_0009000,* ***(B)*** *hsa_circ_0036877,* ***(C)*** *hsa_circ_0111277,* ***(D)*** *hsa_circ_0024157,* ***(E)*** *hsa_circ_0061017,* ***(F)*** *hsa_circ_0054624,* ***(G)*** *hsa_circ_0000284 in maternal blood sampled at 15-16 weeks' gestation from women who went on to have a stillbirth and women who had live births. n = 12 / live births, n = 6 / stillbirth group. Data are presented as mean ± standard deviation. * $p < 0.05$, ** $p < 0.01$, *** $p < 0.001$. Results are considered statistically significant if $p < 0.05$.*

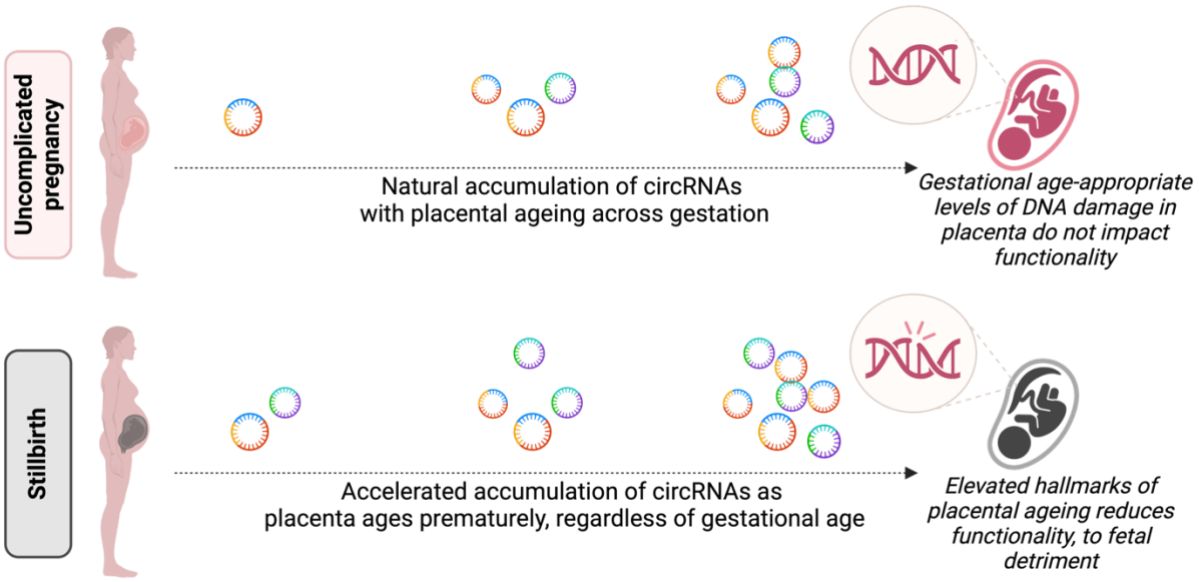

Figure 5. *Proposed mechanism by which circRNA accumulation and placental ageing contribute to stillbirth.*

Supplementary Figure 1. (A-B) *RNA concentration (ng / µL) and* ***(C)*** *abundance (as fold change of RNase R-depleted RNA relative to total RNA) in isolated cells from 37, 38, 39, 40 and 41+ uncomplicated, and stillbirth (S), placentae. n = 12 placentae / uncomplicated gestational group, n = 4 stillbirth placentae. RNA was extracted from each sample, then split into two aliquots; the first was untreated (total RNA) while the second was digested with RNase R (leaving only circRNAs). RNA concentration and abundance of total RNA and RNase R-digested RNA were assessed to determine whether these changed across gestation or in stillbirth. Data are presented as scatter plots with bars and indicate mean ± standard error of the mean. ns = not significant.*

Supplementary Figure 2. *Abundance (as fold change relative to abundance at 37 weeks' gestation) of linear CRHR2 gene variants* ***(A)*** *XM_024446665.1,* ***(B)*** *XM_017011752.2,* ***(C)*** *NM_001202483.2,* ***(D)*** *NM_001202482.2,* ***(E)*** *NM_001202481.1 and* ***(F)*** *NM_001202475.1; linear CWF19L2 gene variants* ***(G)*** *XM_017017239.2,* ***(H)*** *XR_947795.2,* ***(I)*** *NM_152434.3 and* ***(J)*** *XM_011542620.3; linear RAB22A gene variant* ***(K)*** *NM_033109.5; linear FURIN gene variants* ***(L)*** *NM_001382622.1,* ***(M)*** *NM_002569.4,* ***(N)*** *NM_001382619.1,* ***(O)*** *NM_001289823.2,* ***(P)*** *NR_168464.1,* ***(Q)*** *NM_001382620.1,* ***(R)*** *NM_001382621.1 and* ***(S)*** *NM_001289824.2; linear PNPT1 gene variant* ***(T)*** *NM_033109.5; linear PAPPA2 gene variant* ***(U)*** *XM_005245422.3; and linear HIPK3 gene variants* ***(V)*** *NM_001278163.2,* ***(W)*** *NM_001048200.3,* ***(X)*** *NM_005734.5,* ***(Y)*** *XM_04746224.1,* ***(Z)*** *NM_001278162.2,* ***(AA)*** *XM_047426223.1 and* ***(AB)*** *XM_047426225.1 all in isolated cells from 37, 38, 39, 40 and 41+ uncomplicated, and stillbirth, placentae. n = 12 placentae / uncomplicated gestational group, n = 4 stillbirth placentae. Data are presented as scatter plots with bars, and indicate mean ± standard error of the mean. ns = not significant.*